Modeling Blocking Performance with Fragmentation in Spectrally-Spatially Elastic Optical Networks

Imran Ahmed*, Eiji Oki†, *IEEE, Fellow*, and Bijoy Chand Chatterjee*, *IEEE, Senior Member*
*South Asian University, New Delhi, India
†Kyoto University, Kyoto, Japan

***Abstract*—Multi-core and multi-mode fibers (MCMMFs) have been explored to overcome physical limitations and enhance transport capacity. When MCMMFs are combined with elastic optical networks (EONs), they form spectrally-spatially elastic optical networks (SS-EONs), a cutting-edge technology. However, SS-EONs face challenges like fragmentation and crosstalk (XT), which increase blocking probability. Evaluating blocking probability analytically is difficult due to several constraints, leading to one of the most challenging issues in MCMMFs-based SS-EONs. This paper quantifies the fragmentation in SS-EONs while avoiding inter-core and inter-mode XTs simultaneously and computes the blocking probability using a continuous-time Markov chain based analytical model under CMS-RF and CMS-FF policies. The analytical model generates all possible states and transitions while avoiding inter-core and inter-mode XTs for single-class and multi-class requests. Single-class requests use a uniform number of slots, while multi-class requests vary in slot numbers based on client needs. An iterative approximation model for single-hop links is presented when scalability limits the analytical model's tractability. Furthermore, the analytical model is used to evaluate fragmentation for different spectrum allocation policies, including CMS-RF and CMS-FF. Numerical results indicate that the CMS-FF policy results in lower average fragmentation compared to CMS-RF.**

***Index Terms*—Elastic optical network, fragmentation, Markov chain, space-division multiplexing, blocking analysis, crosstalk.**

I. Introduction

Elastic optical networks (EONs) aim to make wavelength-division multiplexing (WDM) networks more efficient by adding flexibility. This flexibility is meant to use spectrum capacity better and reduce waste in single-mode fiber [1]. Despite improving over WDM-based networks, EONs still have limits because of the nonlinear Shannon capacity, which restricts how much information can be sent. Space division multiplexing (SDM) technology utilizes multiple spatial channels for transmitting optical data. Integrating SDM into EONs offers a potential solution to overcome this capacity restriction. SDM utilizes multiple cores, each containing various modes, marking the emergence of spectrally-spatially elastic optical networks (SS-EONs) [2].

When spatial dimensions like core and mode are used in EONs, the routing and spectrum allocation (RSA) problem becomes more complicated. In SS-EONs, RSA turns into the routing, spectrum, core, and mode allocation (RSCMA) problem. RSCMA has two distinct phases: (i) routing and (ii) spectrum, core, and mode allocation in SS-EONs. Six constraints must be followed during RSCMA in SS-EONs: spectrum contiguity, spectrum continuity, core continuity, mode continuity, inter-core crosstalk (IC-XT), and inter-mode crosstalk (IM-XT) constraints, where spectrum, core, and mode conversion are not considered [2]. Continuity constraints require consistent selections of spectrum, core, and mode along the chosen path in routing, while spectrum contiguity constraints demand a contiguous selection of spectrum slots. IC-XT, a significant issue in multi-core fibers (MCFs), occurs when multiple lightpaths share the same spectrum slots in neighboring cores due to evanescent waves. IM-XT happens when adjacent modes in a core use the same spectrum slots for lightpath allocation. Both forms of crosstalk (XT) degrade the quality of transmission and can adversely affect overall network performance [3].

In a dynamic traffic scenario in EONs, when lightpath requests are allocated and released, the network often encounters the generation of isolated free slots, known as spectrum fragmentation. This fragmentation happens because the allocated spectrum slots leave gaps between them, disrupting the spectrum's contiguity and continuity constraints [3]. Inadequate management of spectrum fragmentation can lead to lower utilization of spectrum resources, resulting in an increased blocking of requests in the network. To enhance resource utilization, reducing spectrum fragmentation is essential.

The fragmentation challenge in SS-EONs is even more complex than in EONs due to the added spatial dimensions of cores and modes. Therefore, it is crucial to address fragmentation either by taking preventive measures before lightpaths are established or by making adjustments during lightpath allocation. As fragmentation in the network worsens, the blocking of lightpath requests increases, which negatively affects the overall system performance. Blocking probability (BP), a key performance metric, is calculated by dividing the number of blocked requests by the total number of requests served in the network [4].

The work in [5] presented an accurate analytical model based on a CTMC for SS-EONs, which accurately computes

This work is supported in part by the Core Research grant (Grant Number: CRG/2020/002663), Govt. of India.

979-8-3315-2096-0/25/$31.00 ©2025 IEEE

BP while simultaneously diminishing IC-XT and IM-XT. This model assesses BP considering two distinct allocation policies: core-mode-spectrum random fit (CMS-RF) and CMS-first fit (CMS-FF). However, the research in [5] does not explore how fragmentation affects BP or how to quantify fragmentation using the introduced analytical model.

In this paper, we focus on quantifying fragmentation in SS-EONs while avoiding IC-XT and IM-XT simultaneously, and we compute the BP along with fragmentation in SS-EONs. To calculate BP, we utilize the analytical model based on CTMC from the work [5], which we now refer to as AnfragBP. AnfragBP creates all feasible states and their transitions to compute state probabilities and can handle both single-class and multi-class requests. Single-class requests utilize an identical number of slots, while multi-class requests utilize varying numbers of slots to meet bandwidth demands. AnfragBP calculates BP and fragmentation for the CMS-RF and CMS-FF policies. When AnfragBP is not scalable, we introduce an iterative approximate model focused on the CMS-FF allocation policy for a single-hop link. We compare the average fragmentation and BP of the single-hop model using AnfragBP, the iterative approximate model, and Monte Carlo simulation studies. For the single-hop model, we find that AnfragBP with CMS-FF results in lower BP than with CMS-RF. The BP from AnfragBP and simulation studies are comparable across both allocation policies.

To handle XT in SS-EONs, two approaches are considered: XT-aware and XT-avoided [2], [6]. The XT-avoided approach uses proactive management strategies to prevent XT by ensuring that adjacent cores and modes do not use the same spectrum slots. This approach reduces XT operations and calculations through careful pre-planning. Meanwhile, the XT-aware approach allows the use of the same spectrum slots among adjacent cores and modes if the estimated XT remains below a predefined threshold. While the XT-aware approach enhances resource utilization compared to the XT-avoided approach, it adds complexity to the system [2], particularly with the introduction of multiple modes within a core. For network operators seeking simplified management, the XT-avoided approach is more suitable. This paper focuses on implementing the XT-avoided approach.

TABLE I: Commonly employed symbols

Given parameters:	
X	Set of cores
Y	Set of modes
Z	Set of spectrum slots
W	Set of lightpath request classes
λ_w	Arrival rate of each request in class $w \in W$
μ_w	Service rate of each request in class $w \in W$
c_w	Number of required slots of each request in class $w \in W$
Decision variables:	
A	Set of all states that are generated due to arrival and departure of requests of classes in W
$A_q^{xyw,+}$	Set of feasible states after each request in class $w \in W$ arrives at state $q \in A$, which utilizes mode $y \in Y$ of core $x \in X$
$A_q^{xyw,-}$	Set of feasible states after each request in class $w \in W$ arrives at state $q \in A$, which utilizes mode $y \in Y$ of core $x \in X$
B_w	Set of blocking states for class $w \in W$

II. Analytical Model

This section presents AnfragBP, which systematically creates all conceivable states and their transitions to determine the probability of each state for a single-hop scenario. It uses CMS-FF or CMS-RF policies to assign each request in a class based on combinations of core-mode-slot. The arrival and departure of requests from different classes enable the creation of all feasible states while fulfilling the constraints concerning spectrum contiguity, IC-XT, and IM-XT. Each state's equilibrium equations are derived, and a set of homogeneous linear equations must be solved to obtain the solution. Subsequently, the probability associated with each state is determined, and the BP is computed by aggregating the probabilities of the blocking states. The frequently used notations in the analytical model are defined in Table I. In the following, Algorithm 1 is utilized to describe the process for creating states and identifying transitions between them [5], [7].

Algorithm 1 Generation of state transition diagram

Input: X, Y, W, and Z
Output: State transition diagram
Step 1: Initialize the following sets as empty: A, $A_q^{xyw,+}$, $A_q^{xyw,-}$, and B_w, $\forall x \in X, y \in Y, w \in W$, and $q \in A$.
Step 2: Set A is assigned by an empty state 1.
Step 3: Consider an integer variable q, and it is set to 1 ($q = 1$).
Step 4: While $q \leq |A|$, do the following:
Step 4.1: For $w = 1, \ldots, |W|$, do the following:
Step 4.1.1: If the available slots are greater than the needed slots for a request in class $w \in W$ by fulfilling the constraints of XTs and spectrum contiguity, then:
Add all possible states to $A_q^{xyw,+}$ when each request in class $w \in W$ arrives at state q, which employs mode $y \in Y$ of core $x \in X$.
Step 4.1.2: Else, consider state q as a blocking state for class w.
Set $B_w = B_w \cup \{q\}$.
Step 4.1.3: If $A_q^{xyw,+} \nsubseteq A$, then:
Set $A = A \cup A_q^{xyw,+}$.
Step 4.2: For $w = 1, \ldots, |W|$, do the following:
Step 4.2.1: Add all possible states to $A_q^{xyw,-}$ when each request in class $w \in W$ departs from state q, which employs mode $y \in Y$ of core $x \in X$.
Step 4.2.2: If $A_q^{xyw,-} \nsubseteq A$, then:
Set $A = A \cup A_q^{xyw,-}$.
Step 4.3: Increment w by 1.

In Algorithm 1, we initialize sets A, $A_q^{xyw,+}$, $A_q^{xyw,-}$, and B_w, $\forall q \in A, y \in Y, x \in X$, and $w \in W$ as empty in step 1. An empty state 1 is assigned to set A in step 2. An integer variable q is initialized and set $q = 1$ in step 3. State q endeavors to allocate each request in class $w \in W$ employing mode $y \in Y$ in core $x \in X$ by exploring all combinations of slots, modes, and cores in steps 4.1 to 4.1.3. All states are created as a result of the arrival of each request in class $w \in W$ at state q, employing mode $y \in$

Y in core $x \in X$, while satiating the spectrum contiguity, IC-XT, and IM-XT constraints in step 4.1.1. These feasible states are then included in set $A_q^{xyw,+}$. If a lightpath request in class $w \in W$ fails to fulfill these constraints mentioned above, it is unable to be allocated in state q in step 4.1.2. Consequently, state q is marked as a blocking state for class w, and it is inserted to set B_w. Set $A_q^{xyw,+}$ is checked to see if $A_q^{xyw,+}$ is incorporated in set A in step 4.1.3. If set A does not have $A_q^{xyw,+}$, it is added to set A. New states are created as a result of the departures of each request in class $w \in W$ from state q, employing mode $y \in Y$ in core $x \in X$ in steps 4.2 to 4.2.2. Set $A_q^{xyw,-}$ is examined to see if it is incorporated in set A in step 4.2.2. If set A does not have $A_q^{xyw,-}$, it is inserted in set A. The procedure is reiterated from steps 4 to 4.3 until all states within set A are examined and the overall count of states becomes $|A|$.

Let us examine how states are created using the example in Fig. 1. In this scenario, we have $|X| = 2$, $|Y| = 2$, $|Z| = 4$, and $|W| = 2$. Cores and modes are considered adjacent. Core and mode adjacency is determined using the XT model considered in [3], [5]. The number of required slots for classes 1 and 2 are two and three, respectively, i.e., $c_1 = 2$ and $c_2 = 3$. d denotes IC-XT and IM-XT avoided unutilized slots. According to the CMS-RF allocation policy, each request in class 1 is allocated in mode 1 of core 1 at state 2 with arrival rate $\lambda_1/12$. Similarly, each request in class 2 is allocated in mode 1 of core 1 at state 68 with arrival rate $\lambda_2/8$. During allocation at state 2, IM-XT and IC-XT avoid allocating slots 1 and 2 of mode 2 of core 1 as well as the same slots of mode 1 of core 2. When each request in class 1 departs from state 2, transitions occur with departure rates μ_1. Similarly, when each request in class 2 departs from state 68, transitions occur with departure rates μ_2. Fig. 1 depicts that $|A| = 115$ possible states are produced as a consequence of the arrival and departure of requests in classes 1 and 2. Each dot between states 23 and 112 expresses a state neighbor to at least one of states $i = 1, 2, 3, 23, \cdots, 115$. Due to space constraints, states that are not neighbors to any of those are not shown in Fig. 1.

We present a metric for quantifying fragmentation in each state. It is crucial to differentiate between fragmented slots and crosstalk-avoided unutilized slots, which are utilized to avoid IC-XT and IM-XT. The estimation of fragmentation in each state is determined as follows [3]:

$$F_q = \frac{\sum_{x \in X} \sum_{y \in Y} (1 - \frac{M_{xy}^q}{N_{xy}^q})}{|X| \times |Y|}, \tag{1}$$

where F_q represents the fragmentation in state q. M_{xy}^q is the size of the largest contiguous block of spectrum slots in mode $y \in Y$ of core $x \in X$ in state q. N_{xy}^q is the total number of available spectrum slots in mode $y \in Y$ of core $x \in X$ in state q. We illustrate the fragmentation of a state with an example. For this purpose, we consider state $q = 21$, i.e., (0, 1, 1, 0), (0, d, d, 0), (0, d, d, 0), (0, 1, 1, 0), as shown in Fig. 1. The fragmentation at state $q = 21$ using (1) is estimated as follows: $F_{21} = \Sigma_{1 \in 2} \Sigma_{1 \in 2} (1 - M_{xy}^{21}/N_{xy}^{21}) / |2| \times |2| = (1-1/2)+(1-1/2)+(1-1/2)+(1-1/2) / |2| \times |2| = 0.50$.

The equilibrium equations are developed for SS-EONs considering MCMMFs by [5], [7]:

$$\left(\sum_{x \in X} \sum_{y \in Y} \sum_{w \in W, A_q^{xyw,+} \neq \emptyset} \lambda_{xyw} + \sum_{x \in X} \sum_{y \in Y} \sum_{w \in W, A_q^{xyw,-} \neq \emptyset} g_q \right) \mu_{xyw} \pi_q = \sum_{p \in A, p \neq q} \left(\sum_{x \in X} \sum_{y \in Y} \sum_{w \in W, q \in A_p^{xyw,+}} \frac{\lambda_{xyw}}{|A_p^{xyw,+}|} + \sum_{x \in X} \sum_{y \in Y} \sum_{w \in W, q \in A_p^{xyw,-}} \mu_{xyw} \right) \pi_p, \forall q \in A. \tag{2}$$

In (2), λ_{xyw} signifies a transition rate entering state q through mode $y \in Y$ of core $x \in X$, resulting from the arrival of each request in class $w \in W$. g_q indicates the count of transitions originating from state q, associated with the departure of a request of each class in W. μ_{xyw} represents the transition rate departing from state q through mode $y \in Y$ of core $x \in X$, associated with the departure of each request in class $w \in W$. π_q denotes probability of system being at state q. The outgoing transitions from a state occur when each request in class $w \in W$ using mode $y \in Y$ on core $x \in X$ either arrives or departs. Similarly, the arrival or departure of a request in class $w \in W$ using mode $y \in Y$ on core $x \in X$ triggers incoming transitions. In (2), the left-hand side (LHS) reflects transitions outgoing from state q with probability π_q and the right-hand side (RHS) depicts the transitions that enter state q. The first term on the LHS signifies the transition rate due to the arrival of each request in class $w \in W$ at state q using mode $y \in Y$ of core $x \in X$ with the constraint $A_q^{xyw,+}$ is non-empty. The second term of the LHS refers to the transition rate that occurs from state q, resulting from the departure of each request in class $w \in W$ using mode $y \in Y$ of core $x \in X$ under the condition $A_q^{xyw,-}$ is non-empty. The first term on the RHS reflects the transition rate at which each request in class $w \in W$ arrives in state q. These requests originate from state p that leads to state q using mode $y \in Y$ of core $x \in X$. The second term on the RHS reflects the transition rate at which each request in class $w \in W$ from state p. These requests originate from state p that leads to state q using mode $y \in Y$ of core $x \in X$.

To calculate BP, we analyze the equilibrium equations for all states in the system using any spectrum allocation policy. Additionally, the Markov chain must satisfy a fundamental property that the sum of all state probabilities must be equal to one and expressed by: $\sum_{q \in A} \pi_q = 1$. The equilibrium equations can be derived through the utilization of (2) and the condition $\sum_{q \in A} \pi_q = 1$. We solve these equations to obtain π_q for all $q \in A$. We determine the average BP across all classes by: $\frac{\sum_{w \in W} \sum_{q \in B_w} \lambda_w \pi_q}{\sum_{w \in W} \lambda_w}$. The average fragmentation can be estimated by $U(F_q) \times P$, where $P = [\pi_1, \pi_2, \cdots, \pi_{|A|}]^\top$ is a vector that describes probabilities of all states for a given policy and $U(F_q) = U(F_1), U(F_2), \cdots, U(F_{|A|})$ is a vector with a fragmentation measure based on (1) for each state.

When handling a large number of cores, modes, and spectrum slots, the computational complexity of the introduced analytical model becomes intractable. Therefore, we use an iterative approximate model to evaluate the blocking performance

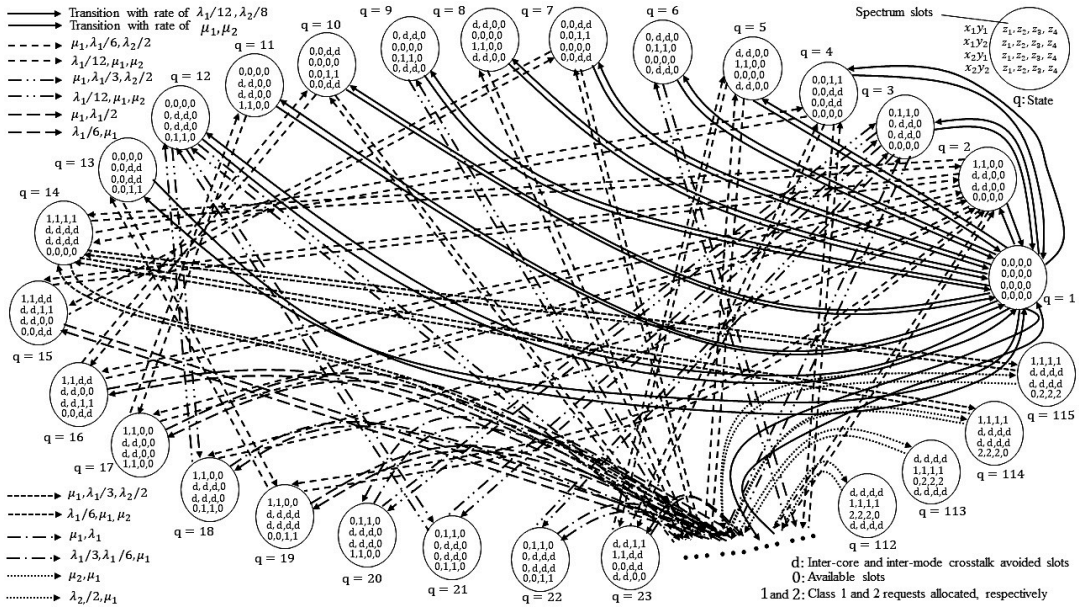

Fig. 1: A portion of state transition diagram considering CMS-RF, where $|X| = 2$, $|Y| = 2$, $|Z| = 4$, $|W| = 2$, $c_1 = 2$, and $c_2 = 3$.

of a link. In this iterative model, allocation follows the CMS-FF policy. This approach offers a computationally manageable alternative for assessing blocking performance in situations where the analytical model's complexity is intractable.

The approximate BP using the iterative approximate model considering all the classes is determined by [5]: $BP = \frac{\sum_{w \in W} \lambda_w (1 - P_1(\alpha, c_w))}{\sum_{w \in W} \lambda_w}$, where $P_1(\alpha, c_w)$ represents the probability of acquiring a minimum of c_w consecutive available slots out of α slots, which is estimated as follows: $P_1(\alpha, c_w) = \sum_{i=1}^{c_w - 1} (P_1(\alpha - i, c_w)(1 - \delta)\delta^{i-1}) + \delta^{c_w}$, for $c_w \geq 1$. α signifies the number of states that corresponds to the total number of slots. The specific value of α is based on the adjacency structure of cores and modes, and the value of α is determined by incorporating crosstalk-avoided unutilized slots in MCMMFs. δ represents the bandwidth utilization ratio for a multi-class case, computed by: $\delta = \frac{1}{\alpha} \sum_{s=1}^{|W|} s P_2(s)$, and for a single-class case ($c_w > 1$), computed by: $\delta = \frac{1}{\alpha} \sum_{s=c_w}^{|W|} s P_2(s)$. $P_2(s)$ is the probability of states with an allocation of s slots, determined as follows: $P_2(s) = \frac{\sum_{w=1}^{|W|} c_w \left(\frac{\lambda_w}{\mu_w}\right) P_2(s - c_w)}{s}$. Here, $P_2(s) = 0$ if $s < 0$, and $P_2(0) + \sum_{s=1}^{\alpha} P_2(s) = 1$ if $s \geq 1$.

III. Performance Evaluation

We evaluate and compare the performance of AnfragBP in terms of average fragmentation using (1) under the CMS-FF and CMS-RF policies for a link. Further, we compare the performance of AnfragBP, iterative approximate model, and Monte Carlo simulations in terms of BP using the CMS-FF and CMS-RF policies for a link. Lightpath requests are generated according to a Poisson distribution with an average rate λ, each request being independent. Request service times follow an exponential distribution with an average of μ^{-1}. Incoming requests are uniformly distributed among $|W|$ classes, with $\lambda_w = \frac{1}{|W|}\lambda$ and $\mu_w = \mu$ for all $w \in W$. The load is defined as $\frac{\lambda}{|W|\mu}$. The study investigates three main approaches: (i) AnfragBP encompassing CMS-FF and CMS-RF policies, named AnfragBP (CMS-RF) and AnfragBP (CMS-FF), (ii) Monte Carlo simulation studies, including CMS-FF and CMS-RF policies, named Sim (CMS-RF) and Sim (CMS-RF), and (iii) an iterative approximate model employing the CMS-FF policy for allocation, named Approximation.

Table II compares average fragmentation using (1) and AnfragBP under different load for a single-class case with $|X| = 2$, $|Y| = 2$, $|W| = 1$, and $|Z| = 10$ and multi-class case with $|X| = 2$, $|Y| = 2$, $|W| = 4$, and $|Z| = 8$. In a single-class case, we find that AnfragBP with the CMS-FF policy leads to less fragmentation compared to using CMS-RF. This pattern is also observed in the multi-class case, where AnfragBP with CMS-RF results in higher fragmentation than AnfragBP with CMS-FF. The reason is that CMS-FF allocates resources in a way that maximizes the number of available cores on any spectrum slots and modes for future requests, which leads to an increase in the number of available slots.

Figure 2 (a) compares BP among AnfragBP, Approximation, and Sim for a single-class case with $|X| = 2$, $|Y| = 2$, $|W| = 1$, and $|Z| = 10$. As load increases, BP rises due to rises in the arrival rate of requests. We find that the CMS-FF policy outperforms the CMS-RF policy by showing a lower BP in both AnfragBP and Sim. This is because the CMS-RF policy typically has more states when using AnfragBP than the CMS-FF policy. Additionally, CMS-RF leads to more blocking states due to increased spectrum fragmentation, which explains why AnfragBP with CMS-RF has a higher BP than with CMS-FF. Fig. 2 (b) compares BP among AnfragBP, Approximation, and Sim for a multi-class case with $|X| = 2$, $|Y| = 2$, $|W| = 4$, and $|Z| = 8$. Similar to a single-class case, in a multi-class case, we observe that AnfragBP and Sim with the CMS-RF policy have

TABLE II: Comparison of average fragmentation using (1) and AnfragBP for different load.

Approaches	$\|X\|=2, \|Y\|=2, \|W\|=1$, and $\|Z\|=10$					$\|X\|=2, \|Y\|=2, \|W\|=4$, and $\|Z\|=8$				
	Load					Load				
	0.2	0.4	0.6	0.8	1.0	0.2	0.4	0.6	0.8	1.0
AnfragBP (CMS-RF)	0.0302	0.0567	0.0797	0.0994	0.1159	0.0966	0.1384	0.1546	0.1594	0.1631
AnfragBP (CMS-FF)	0.0262	0.0483	0.0664	0.0812	0.0929	0.0730	0.1003	0.1080	0.1098	0.1152

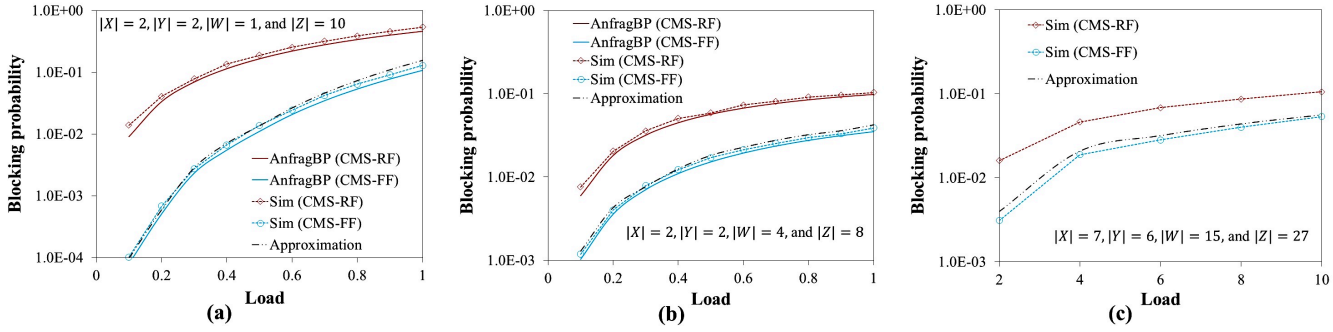

Fig. 2: Comparison of blocking probability using different approaches: (a) single-class case, (b) multi-class case, and (c) multi-class case with large-scale scenario.

higher BP than AnfragBP and Sim with the CMS-FF policy. We also observe that the results of Approximation, AnfragBP, and Sim with the CMS-FF policy are close and show a similar trend. Fig. 2 (c) compares BP using Approximation and Sim for a large-scale scenario with $|X| = 7$, $|Y| = 6$, $|W| = 15$, and $|Z| = 27$. The results of Sim using CMS-FF show lower BP than that of CMS-RF. Additionally, Approximation closely mirrors Sim with CMS-FF trends, validating its effectiveness in reflecting real-world scenarios.

IV. Conclusion and Future Direction

This paper evaluated the fragmentation in SS-EONs while avoiding IC-XT and IM-XT simultaneously and computed the blocking probability using a CTMC-based analytical model under CMS-RF and CMS-FF policies. The analytical model creates all feasible states and their transitions to determine state probabilities while considering IC-XT and IM-XT simultaneously. For scalability issues in single-hop links, an iterative approximate model was presented. Numerical results showed that the analytical model using CMS-FF has lower average fragmentation than an analytical model with CMS-RF. We found that the BP of the analytical model with CMS-FF is lower than that of an analytical model with CMS-RF due to the lower fragmentation of CMS-FF. Additionally, results from simulation studies with CMS-FF and the iterative approximate model exhibited similar trends and were closely aligned.

To calculate the average fragmentation in a network, we can follow the approach given by [3]. The fragmentation in the network, denoted by γ, is given by $\gamma = 1 - \phi$, where ϕ represents the ratio of contiguous-aligned available slots across the network for all routes associated with each established request in class $w \in W$. Specifically, ϕ is calculated as $\phi = \sum_{w \in W} \sum_{r \in R_w} \beta_r^w \xi_r^w$ and $\xi_r^w = \frac{\psi_r^w}{|Z|}$. Here, β_r^w denotes the weight of route $r \in R_w$ for each request in class $w \in W$, which is defined by $\beta_r^w = \frac{1}{|Z| \times |R_w|}$, and ψ_r^w is the maximum number of contiguous-aligned available slots in the core and mode used by route $r \in R_w$ for an established request in class $w \in W$. R_w refers to the set of routes for each request in class $w \in W$. The number of contiguous-aligned available slots for a request indicates the total available slots that are contiguous and aligned along the route. Future work will address the evaluation of average fragmentation in the network.

References

[1] M. Jinno, H. Takara, B. Kozicki, Y. Tsukishima, Y. Sone, and S. Matsuoka, "Spectrum-efficient and scalable elastic optical path network: Architecture, benefits, and enabling technologies," *IEEE Commun. Mag.*, vol. 47, no. 11, pp. 66–73, 2009.

[2] H. Tode and Y. Hirota, "Routing, spectrum, and core and/or mode assignment on space-division multiplexing optical networks," *IEEE/OSA J. Opt. Commun. Netw.*, vol. 9, no. 1, pp. A99–A113, 2017.

[3] B. C. Chatterjee, A. Wadud, and E. Oki, "Proactive fragmentation management scheme based on crosstalk-avoided batch processing for spectrally-spatially elastic optical networks," *IEEE J. Sel. Areas Commun.*, vol. 39, no. 9, pp. 2719–2733, 2021.

[4] H. Beyranvand, M. Maier, and J. A. Salehi, "An analytical framework for the performance evaluation of node-and network-wise operation scenarios in elastic optical networks," *IEEE Trans. Commun.*, vol. 62, no. 5, pp. 1621–1633, 2014.

[5] I. Ahmed, R. K. Rai, M. Maity, E. Oki, and B. C. Chatterjee, "AnalyticalBP: Analytical model for blocking probabilities considering crosstalk-avoided approach in spectrally-spatially elastic optical networks," *IEEE Trans. Commun.*, vol. 72, no. 3, pp. 1487 – 1501, 2023.

[6] M. Yang, Y. Zhang, and Q. Wu, "Routing, spectrum, and core assignment in SDM-EONs with MCF: node-arc ILP/MILP methods and an efficient XT-aware heuristic algorithm," *IEEE/OSA J. Opt. Commun. Netw.*, vol. 10, no. 3, pp. 195–208, 2018.

[7] S. K. Singh and A. Jukan, "Computing blocking probabilities in elastic optical networks with spectrum defragmentation," in *Proc. INFOCOM*, Paris, France, 2019, pp. 424–432.